Icarus **144**, 353–366 (2000)
doi:10.1006/icar.1999.6303, available online at http://www.idealibrary.com on IDEAL®

Microtektites on Mars: Volume and Texture of Distal Impact Ejecta Deposits

Ralph D. Lorenz

Lunar and Planetary Laboratory, Department of Planetary Sciences, University of Arizona, 1629 East University Boulevard, Tucson, Arizona 85721-0092
E-mail: rlorenz@lpl.arizona.edu

Received January 25, 1999; revised November 22, 1999

Microtektites, small blobs of ejecta formed in the shock melt and vapor plume of an impact, can be dispersed far from the source crater only if the impact is violent enough for the ejecta plume to pierce the atmosphere; they are therefore formed in far smaller (and more numerous) impact events on Mars than on Venus and Earth, which have thicker atmospheres. Microtektite abundances from the Chicxulub and Bosumtwi craters on Earth suggest that the volume of this material is $\sim 5 \times 10^{-5} D_c^{3.74}$ km^3, with D_c the crater diameter in kilometers, similar to the observed volumes of the dark parabolic ejecta deposits on Venus. Corresponding volumes on Mars are $\sim 2.5\times$ smaller, but even so this result implies that even only a 15-km crater can produce a layer of microtektites with a global average thickness on Mars of 40 microtektites per square centimeter. I use a trajectory code and a thermal model to show that these particles are easily dispersed globally on Mars and that micrometeoroids of the same size will be unmelted by reentry heating. The uniform size and glassy texture of microtektites may allow such ejecta layers to be identified by the remote arm cameras on Mars landers, particularly in the polar layered terrain where they may be preserved against abrasion.

Key Words: **Impact Processes; Mars, Surface; Mars, Atmosphere; Meteorites.**

INTRODUCTION

Impacts and nuclear explosions on Earth create tiny molten particles of rock-variously termed microtektites, microkrystites, and spherules (see, e.g., Glass 1990 and Grieve and Shoemaker 1994). In the largest events, these particles can be distributed worldwide, although for craters less than a few kilometers on Earth, the atmosphere confines them to the vicinity of the crater. Such small particles are easily dissolved and lost from the geological record and are so far known to be associated with a handful of terrestrial craters. Widespread ejecta deposits of small particles are, however, also seen around the most recent craters on Venus.

In this paper, I show that consideration of the formation mechanism and observed thicknesses of these terrestrial and Venusian deposits implies that they should form in abundance on Mars as well. They furthermore may be well-preserved in the martian polar terrain, and thus visible to the remote arm cameras on the present (1998–2001) generation of Mars landers. It may be that the spoor of catastrophe lurk in their thousands in every scoop of dirt on Mars, attesting to violent events in Mars' history.

Such layers may well prove to be useful as analogs of volcanic horizons in terrestrial ice deposits which form both a record of the volcanic events themselves and a date reference within the ice column to correlate with stratigraphic records elsewhere. Impact ejecta, trapped pristine in polar ice, may provide useful information on the impact itself: the mineralogy may be indicative of the composition of the impactor, its thickness variation may point to the source crater, and the size distribution and morphology of the individual particles may shed light on the impact process itself.

Since impact ejecta is deposited more-or-less instantaneously, compared with the steady infall of interplanetary dust particles (IDPs), they may form a compositionally uniform layer of significant thickness. I show that significant layers are likely to be present by comparing the expected cratering rate coupled to simple relations for the thickness of the corresponding deposits with the probable age of the ice caps and layered terrains.

Impact ejecta particles, by definition on suborbital trajectories, will have different entry velocities, and therefore different thermal histories, from micrometeorites arriving on hyperbolic orbits. I show that the fraction of particles that are melted for different size ranges may therefore allow a simple and independent confirmation of impact origin of a layer.

MARTIAN POLAR DEPOSITS

The two principal terrains particular to the martian polar regions are the polar layered terrain and the ice caps themselves (e.g., Thomas *et al.* 1992, Blasius *et al.* 1982). The layered terrain, as the name suggests, comprises layers at least as thin as a few meters, apparently of mixed dust and ice of varying proportions.

Plaut *et al.* (1988) present a count of 15 craters on the southern layered terrain, and determine that the terrain is at least 100 Myr

0019-1035/00 $35.00

old. However, as Thomas *et al.* (1992) point out, some of these craters may be exhumed and the terrain may be correspondingly younger. Cutts *et al.* (1976) found no craters >300 m in diameter in the northern layered terrain, suggesting an age (Thomas *et al.* 1992) of 10 Myr or less. Crater numbers and resurfacing rates are also discussed in Herkenhoff *et al.* (1997). Ice and dust deposition-rate calculations, summarized in Thomas *et al.* (1992) can place a likely lower age limit—a 30-m layer of ice could be deposited in about 10^5 years—but are somewhat uncertain. The caps have apparent topography of the order of a few kilometers (Zuber *et al.* 1998) and so are probably of the order of 10 Myr old if this deposition rate applied, although the age of the present cap configuration probably relates to the $\sim 10^5$-year spin axis variation.

The non-ice component of the polar caps and layered terrain may be expected to comprise four principal components. The first, and generally the only one to be considered, is dust from elsewhere on Mars transported in atmospheric suspension and either settled out naturally or precipitated by condensation of water or CO_2 ice. Optical measurements from the Pathfinder lander (Tomasko *et al.* 1999) suggest these particles are around 1.6 μm in diameter: larger particles sediment out quickly. Although regional dust deposition rates may be as high as 400 μm per year (Moersch *et al.* 1999) in Mars' more dynamic regions where surface albedo and thermal changes have been observed from Earth, the global average, and polar regional, deposition rates are likely to be much lower.

A second component is silt-sized particles blown along the ground (saltated) by winds: during winter, when there is net deposition onto the cap, net winds are poleward. However, this process is probably very weak in depositional terms onto the poles, since such winds would need to be strong to transport large particles, especially uphill. Indeed, Thomas and Gierasch (1995) have determined that dunes in the margins of the northern martian pole reflect a steady dispersal of material *from* the pole.

The third component, and one present in notable quantities in terrestrial polar ice deposits, is meteoric material. Flynn and McKay (1990) have noted that the martian soil may contain a significant amount of meteoric material and that the polar deposits in particular may be particularly rich in these materials. A fourth component, largely undiscussed in the literature to date, and the principal subject of this paper, is ejecta from large impacts elsewhere on Mars.

Terrestrial ice sheets are well known as fertile hunting grounds for IDPs and meteorites. However, on Earth, the thick atmosphere and high gravity conspire to make impacts capable of dispersing ejecta globally fairly rare, and the ice sheets themselves are young, so there are no known impact ejecta layers in the ice. It is, however, believed that marine diatoms found on the ice-free Transantarctic Mountains may have been emplaced there as ballistic ejecta from the >1-km-diameter Eltanin asteroid impact in the Southern Ocean 2.15 Myr ago (Gersonde *et al.* 1997, Smit, 1997).

EXOATMOSPHERIC EJECTA DISPERSAL—ATMOSPHERE-PIERCING IMPACTS

On bodies with atmospheres, impact ejecta is generally confined to the immediate vicinity of the crater. To clarify the discussion that follows, a distinction must be drawn between two components of impact ejecta. The most voluminous material that typically makes up the visible ejecta blankets around craters is rock excavated by the cratering flowfield and is only modestly altered by the impact; on Mars many ejecta blankets have a lobate appearance (e.g., Strom *et al.* 1992) probably due to the effects of subsurface ices. A much smaller amount of material, comprising material from the projectile as well as the target, is heated dramatically by the impact event and forms a fireball. It is this material that forms the subject of this paper.

In small impacts, this fireball expands only slightly before equilibrating in pressure with the atmosphere: buoyant due to its high temperature, it rises and turns into a mushroom cloud. Fine ejecta particles of molten material, or condensed rock vapor, are carried upward in the cloud and may be dispersed into a streak downwind.

However, if the impact is sufficiently energetic, the explosion will puncture the atmosphere (see, e.g., Melosh 1989, Vickery and Melosh 1990, Toon *et al.* 1997, Adushkin and Nemchinov 1994) and ejecta can be dispersed ballistically above the atmosphere and reenter at great distance from the crater. The puncture can occur only if the expanding fireball caused by the impact has sufficient energy that its radius (were it to expand to ambient conditions) exceeds a scale height, such that the fireball can "sense" the top of the atmosphere and continue to expand vertically. Vervack and Melosh (1992) express the minimum projectile diameter D_p that can cause such an explosion as

$$D_\mathrm{p} = 2H \cdot \left(\frac{P_0}{S \rho_\mathrm{p} V_\mathrm{i}^2} \right)^{1/3\gamma}, \qquad (1)$$

with γ the ratio of specific heats (1.4 for N_2, 1.66 for CO_2), V_i the impact velocity, H the scale height of the atmosphere, P_0 the surface atmospheric pressure, and ρ_p the mass density of the impactor. S is a factor related to the target material (Melosh 1989) and is $\sim$1.3 for rock. The resultant D_p values for Venus, Earth, and Mars are approximately 1400, 400, and 300 m assuming typical impact velocities of 21, 18, and 12 km/s, respectively (e.g., Grieve and Cintala 1998), and $H = 8000$ km and $\rho_\mathrm{p} = 2600$ kg/m^3. The lower impact speeds somewhat offset the thinner atmospheres of Earth and Mars in lowering the threshold impactor size, but the atmospheric pressure is by far the dominant effect.

The size of crater formed by such an impact can be estimated from crater scaling laws. Following Grieve and Cintala (1992) and Strom *et al.* (1992) and others, I use the transient cavity formulation in cgs units due to Schmidt and Housen (1987),

$$D_\mathrm{tc} = 1.16 \left(\frac{\rho_\mathrm{P}}{\rho_\mathrm{t}} \right)^{0.33} D_\mathrm{p}^{0.78} V_\mathrm{i}^{0.44} g^{-0.22}, \qquad (2)$$

with D_{tc} the diameter of the transient cavity, ρ_t the density of the target, g local gravitational acceleration, and other symbols defined as before. The resultant crater rim diameter D_r is estimated by the expression due to Croft (1985),

$$D_{tc} = D_Q^{0.15} D_r^{0.85}, \quad (3)$$

where D_Q is the simple-to-complex transition diameter, which depends on target properties and gravity: here I use 4 km for Venus, Earth, and Mars (the 0.15 exponent makes results fairly insensitive to the assumed value). Thus a 300-m impactor on Mars at 12 km/s will produce a 2.7-km-diameter crater. Craters of this size and larger will puncture the atmosphere and produce strewn fields of microtektites.

Vervack and Melosh (1992) showed how ejecta distributed by an atmosphere-piercing ejecta plume could account for the dark parabolic features associated with some impacts on Venus (see Fig. 1). They found that the parabolic features could be reproduced by a model of re-entrant ejecta, with a mean size falling off with distance from the impact, being winnowed by zonal winds. The ejecta is initially deposited with circular symmetry around the source crater at the top of the atmosphere. Since small

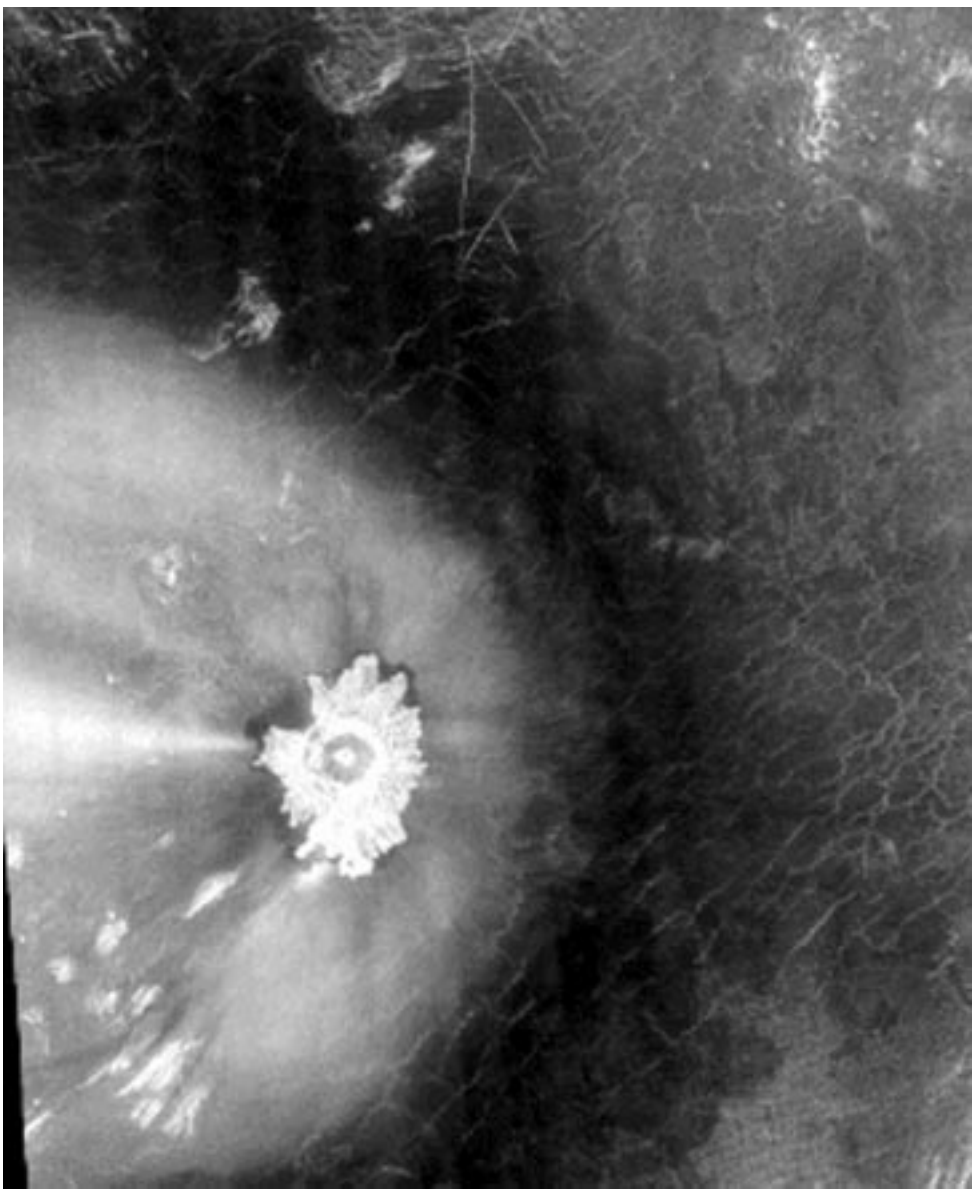

FIG. 1. Parabola on Venus formed by ejecta deposited above the atmosphere in an initially circularly symmetrical pattern, then winnowed eastwards by zonal winds. The inner region is bright due to blockier ejecta: the dark parabola is poorly radar-backscattering, requiring a thickness of several centimeters of fine ejecta. Source is the crater Adivar at the center (8.93°N, 76.22°E, 30 km across). The parabola shown is intermediate in size between the north and south polar caps on Mars. Magellan Image F-MIDR-10N076. Black stripe is missing data.

ejecta falls slower, its horizontal displacement by wind is larger, smearing the circular shape into a parabola.

The radar-dark parabolae require smooth (or radar-absorbing) ejecta deposits several centimeters thick, probably comprising particles down to about 200 μm diameter. Smaller particles will be more widespread, but are invisible to remote sensing at these centimeter wavelengths (and are more easily removed by wind in any case).

The impactor sizes calculated above imply that events on Mars and Earth forming craters of only a few kilometers diameter will pierce the atmosphere and distribute ejecta ballistically beyond. On Venus, craters must be somewhat larger for this to occur; from Eqs. (1)–(3), they need to be ~12 km. Schaller and Melosh (1998) survey craters with ejecta parabolas: all but 3 of the 58 such craters identified in Magellan data have diameters above 10 km, essentially consistent with this limit.

On Earth, no parabolas are known, but fields of microtektites have been identified in deep-sea sediments, notably the Ivory Coast tektites associated with the Bosumtwi crater and the Australasian microtektites, associated with a yet-to-be-discovered impact crater, most probably located in Southeast Asia (see, e.g., Glass and Pizzuto 1994). It may be noted that microtektites are associated with moderately recent impacts, in that fine material is easily weathered and altered on Earth . Because of the need to pierce the atmosphere for their widespread distribution, they are also only associated with large impacts (craters above about 5 km in diameter). Impacts that are both large and recent are moderately rare, so few strewn fields are known, although as Grieve and Shoemaker (1994) suggest, a determined search might find many more.

VOLUME OF MICROTEKTITE DEPOSITS: INSIGHTS FROM EARTH AND VENUS

Although there is no a priori reason to expect it to work for microtektite ejecta distant from the source crater, since the mode of formation and emplacement is different, the expression for the thickness of near-field ejecta derived for lunar craters by McGetchin *et al.* (1973) has been used with some success to reproduce the thickness of terrestrial microtektite ejecta deposits. This relation may be expressed in a general form,

$$t = kR_C^x \cdot \left(\frac{R_C}{r}\right)^n, \tag{4}$$

where r is the distance from the center of the crater, whose radius is R_C ($=D_r/2$), k is a constant, as are exponents x and n. McGetchin *et al.* (1973) have $k = 0.14$, $x = 0.74$, and $n = 3$, with dimensions in meters. Other related expressions exist, for example that due to Stoffler *et al.* (1975) with $k = 0.06$, $x = 1$, $n = 3.3$. Glass and Pizzuto (1994) fit the observed abundances of Australasian microtektites (for which the size and location of the source crater are unknown) with $k = 0.02$, $x = 0$, $n = 4.4$. Measurements by the Mars Orbiter Laser Altimeter (MOLA) (Garvin and Frawley 1998) of the topographic profiles of the ejecta blankets around 98 craters on Mars have been fit with $x = 0$ and n over the wide range of -2 to $+17$, probably indicating a wide range of target materials.

The Stoffler *et al.* and McGetchin *et al.* expressions successfully predict the abundance of microtektites in the Ivory Coast field, generated by the 10.5-km Bosumtwi crater. The counts (from Glass and Pizzuto 1994), are presented in Fig. 2a with a number of candidate fits.

Hildebrand and Stansberry (1992) found that the ejecta thickness from the Chicxulub (K/T) impact was described well by this relation from just over 100 km to several thousand kilometers from the crater center. The relation would predict a thickness of ~100 μm at a range of 10,000 km. In fact, a deposit of spherules was found in the Pacific Ocean sediments at this distance—so far from the Yucatan, indeed, that it was not at first believed to be associated with the Chicxulub impact (Robin *et al.* 1993). This deposit was inferred to have a fluence of 40–140 mg cm^{-2}: taking a density of 2600 kg m^{-3} gives an equivalent thickness of 150–500 μm—a quite reasonable agreement, especially given the possible effects of ocean currents and the uncertainties introduced by plate reconstruction. Figure 2b shows the various expressions again, together with data from the compilation by Hildebrand (1992) and the datapoint from Robin *et al.* (1993).

Again, the Stoffler *et al.* (1975) and the McGetchin *et al.* (1973) expressions work well, with the latter perhaps fractionally better overall. For the remainder of the paper, we retain the McGetchin *et al.* (1973) parameters, although Stoffler parameters could be used with little difference in results.

Equation (4) may be integrated between some minimum radius R_m and infinity to yield the volume of ejecta produced:

$$V_{ejecta} = \frac{2k\pi}{1-n} R_C^{n+x} R_m^{2-n}. \tag{5}$$

For the ejecta to be dispersed above the atmosphere, R_m is presumably commensurate with the height at which the ejecta particles are no longer affected by drag—roughly 100 km for Earth and Venus, perhaps a little lower for Mars. It should be noted that for $n < 2$ (and thus for roughly half of the craters measured by Garvin and Frawley (1998)) the integral does not converge. Applying the McGetchin *et al.* values and $R_m = 100$ km, (5) becomes

$$V_{ejecta} = 7.3 \times 10^{-4} R_C^{3.74} = 5 \times 10^{-5} D_r^{3.74}, \tag{6}$$

with the volume in km^3 and the radius R_C or diameter D_r in kilometers.

Since the microtektite ejecta is produced in and dispersed by the plume of high temperature material in the impact event, it is interesting to compare the relation above to that determined by Grieve and Cintala (1992) for the volume of impact melt. They used a model of the propagation of impact shock and equations of state to evaluate the amount of melt produced. They also compared the resultant volumes with those measured on the geological investigation of several terrestrial craters. Over six orders

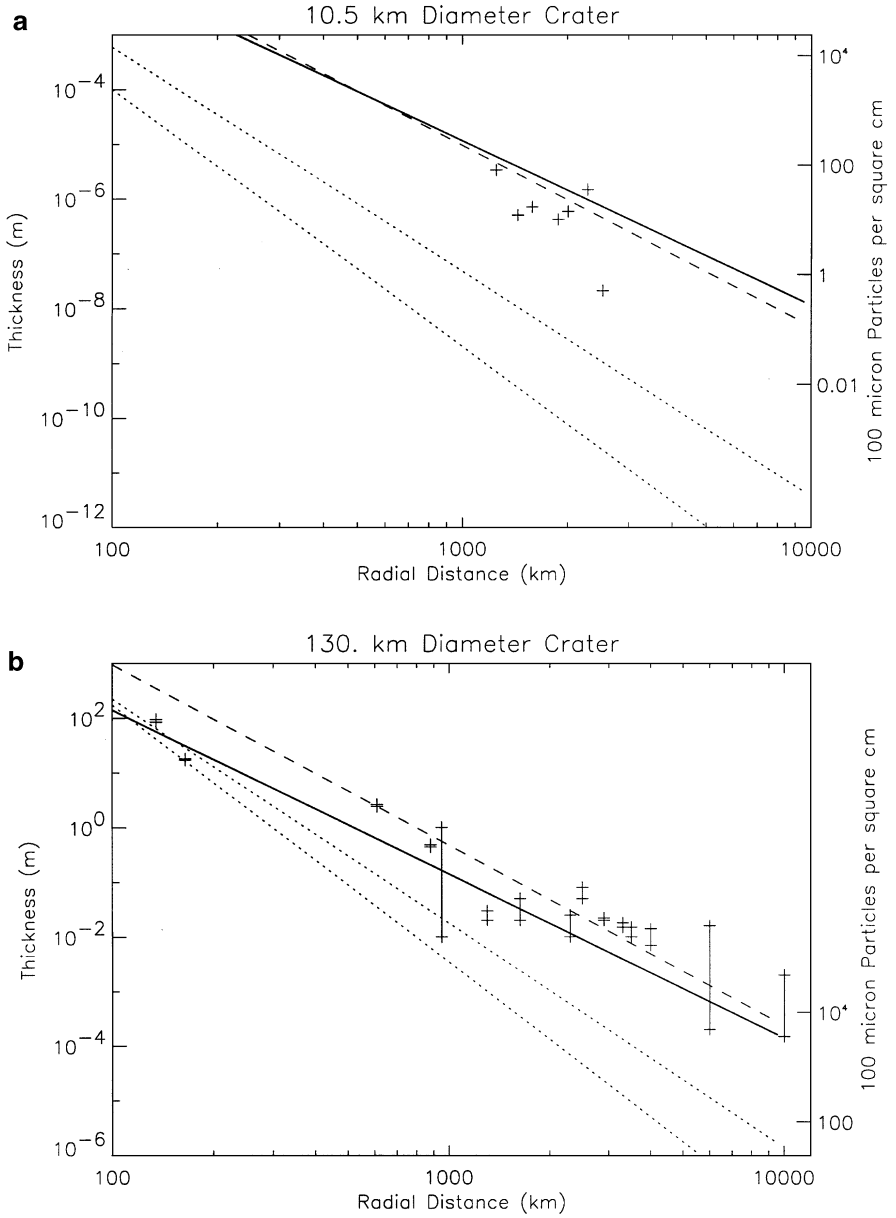

FIG. 2. (a) Thickness of ejecta deposit as a function of distance from a 10.5-km-diameter crater. Dotted lines are the regression limits (Glass and Pizzuto 1994) for the Australasian microtektite crater (although the source crater for these deposits is probably rather larger than 20 km diameter). Right axis gives the layer depth as an equivalent mass of 100-μm-diameter particles. The crosses are microtektite counts at various distances from the 10.5-km Bosumtwi crater (Glass and Pizzuto 1994). The solid line is the preferred relationship due to McGetchin *et al.* (1973) and the dashed line that due to Stoffler *et al.* (1975). (b) As (a), for the K/T ejecta from the Chicxulub crater. Data (crossed vertical bars to denote range of values) from Hildebrand (1992) and Robin *et al.* (1993).

of magnitude of melt volume (from 10^{-2} to nearly 10^4 km^3) they found

$$V_{\text{melt}} = 7.1 D_{\text{tc}}^{3.85}, \tag{7}$$

with the factor increasing slightly with impact velocity and impactor density. Units are km^3 and kilometers. Combining Eqs. (3) and (7) yields

$$V_{\text{melt}} = 6.8 \times 10^{-3} R_{\text{C}}^{3.27}. \tag{8}$$

This expression is strikingly similar in form to the expression (6) for microtektite volume, as would be expected from the common circumstances of melt pool and microtektite formation. For craters with radii of 1–50 km, the distal ejecta volume is respectively 1/10th to one half of the volume of local impact melt.

We may gain added confidence in using Eqs. (4) and (6) to predict distal ejecta thickness by examining the parabolic ejecta deposits on Venus. Although the thickness of these deposits was not measured directly by Magellan's radar, an average thickness for each deposit was computed by Schaller and Melosh (1998),

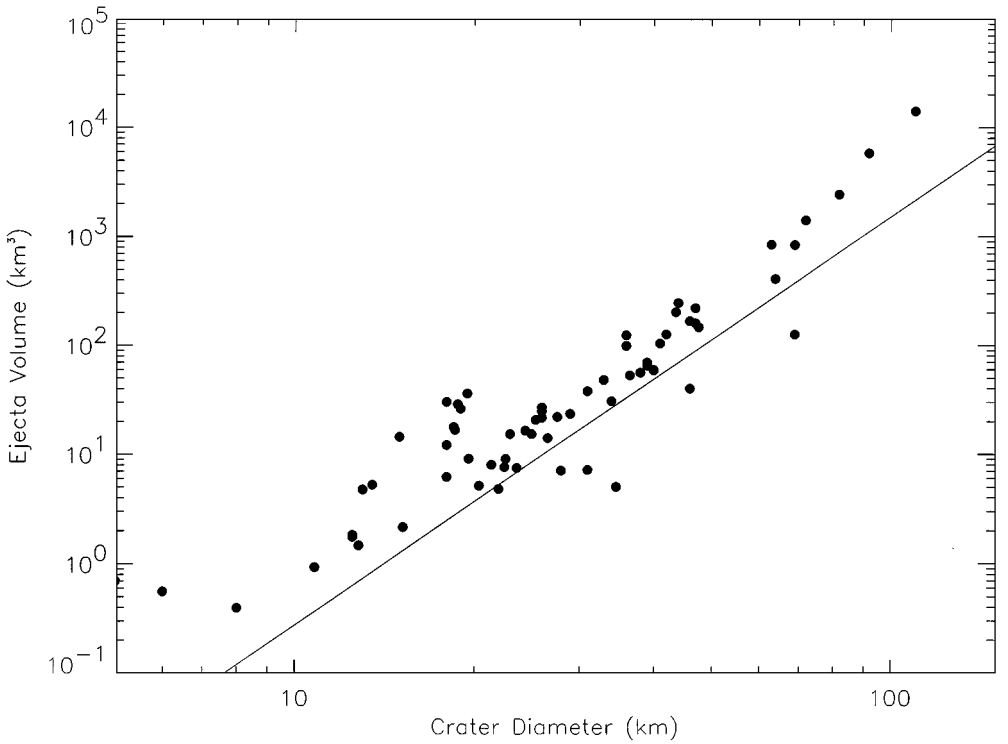

FIG. 3. Volume of parabolic ejecta deposits on Venus (dots) as a function of source crater size. The line denotes volume estimated from Eq. (6) in the text—it reproduces the trend of the data very well, although with a consistent underestimation of ~2.

who fit the shapes of the deposit with a model of ejecta dispersal. I combine this thickness estimate (ranging from less than a centimeter to several meters) with the area of each deposit as measured by Campbell *et al.* (1992) to determine the ejecta volume.

The results for the 67 features on Venus are plotted against the parent crater diameter in Fig. 3 and compared to Eq. (6). It can be seen that the trend of the data is well-reproduced by Eq. (6)—apparently McGetchin *et al.* (1973)underpredict the thickness by only a factor of about 2. In fact, since impact velocities at Venus are slightly higher, and the surface of Venus is closer to the melting temperature of rocks than is the Earth, one might reasonably expect that the melt and ejecta volumes would be larger than for the same size crater on Earth.

Finally, Toon *et al.* (1994) note that the dust in the plumes of large nuclear explosions, produced in a similar way to melt droplets in impacts, but perhaps supplemented somewhat by swept-up surface materials, is generally around 0.3×10^9 kg/megaton ($1\ \mathrm{MT} = 4.2 \times 10^{15}$ J). Zahnle (1990) similarly showed that a typical terrestrial impact should have a dust yield of about 0.1×10^9 kg/megaton. Since the diameter of an explosion crater may be related to the energy E (SI units) by, e.g., Hughes (1999),

$$E = 3.03 \times 10^6 D_{\mathrm{r}}^{3.38}. \tag{9}$$

It follows for the latter dust yield that the fine/molten ejecta volume is approximately

$$V_{\mathrm{ejecta}} = 3.8 \times 10^{-4} R_{\mathrm{C}}^{3.38}, \tag{10}$$

with ejecta volume in km^3 and R_{C} in kilometers. Despite the independent and empirical derivation of this result, it is remarkably similar to equation (6).

APPLICABILITY TO MARS

The McGetchin *et al.* (1973) formulation and a fraction of a similar expression for melt volume appear to successfully estimate the volume of distal ejecta deposits on Venus and Earth, two planets with similar size and gravity. It does not necessarily follow that the dependence of thickness on distance follows the same law on much smaller Mars. Making the "flat Earth" approximation and ignoring atmospheric drag, a particle at speed V will travel a maximum distance $\sim V^2/g$—or about 2.6 times as far on Mars as on Earth or Venus.

Microtektites are accelerated by the expansion of the ejecta plume, and thus their dispersal speed relates to the energy of the plume and thus the kinetic energy of the impactor. Melosh and Vickery (1991) suggest that the maximum velocity of the expanding plume is $\sim V_{\mathrm{i}}/2$. Consideration of the distance covered by K/T ejecta (10,000 km—see Fig. 4) and the implied ejecta velocity suggests $V_{\mathrm{i}} \sim 20$ km/s, a reasonable number.

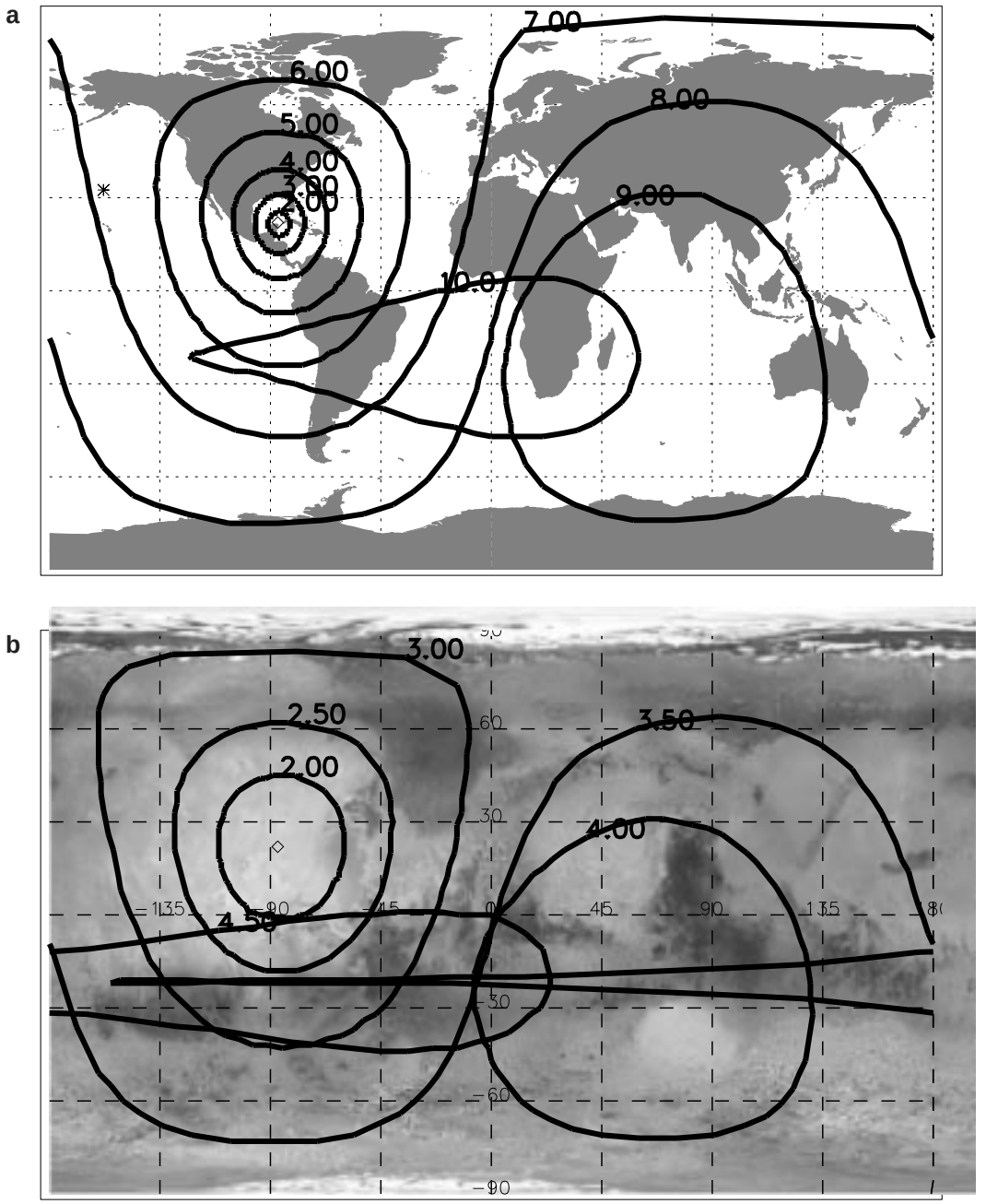

FIG. 4. Loci of impact points for ejecta launched at various velocities (i.e., the contours show the launch speed in km/s, required to reach a given distance) at an elevation of 45° from a crater at 22°N, 87°W, indicated by a diamond, on Earth and Mars. (a) Earth—access to the poles requires a launch velocity of around 7 km/s, while global coverage requires around 10 km/s; such trajectories are appreciably smeared by Earth's rotation into a teardrop shape. The asterisk denotes the K/T debris recovered by Robin *et al.* (1993) (b) Mars—the picture is similar, but the caps are reached by ejecta launched at 3.5 km/s, while global distribution requires only around 4.5 km/s. The flight time of such trajectories on Mars is more than one sol—the teardrop is stretched around the planet nearly one and a half times.

Mars, being further from the Sun than Earth and Venus, and with a lower escape velocity, thus has a lower typical impact velocity ∼12 km/s, compared with 18 and 21 km/s, respectively (Grieve and Cintala 1998). It follows then that ejecta on Mars in general is accelerated to around 50–70% of the corresponding velocities—more or less exactly cancelling out the effect of the lower gravity on the range of ejecta. Thus the distance dependence of thickness should be roughly the same for Mars and Earth.

The total fine ejecta volume, however, should be sensitive to impact velocity, as is melt volume. Cintala and Grieve (1991) show that the melt volume as a fraction of the transient cavity

volume is about a factor of 2.5 lower for Mars than Earth and Venus, and Clifford *et al.* (1991) quote the result as $2.14 \times 10^{-5} D_{\mathrm{tc}}^{3.83}$. If we scale the fine ejecta volume by the same factor, we should take parameters $k = 0.05, x = 0.74, n = 3$ for applying Eq. (4): these parameters are used in the rest of this paper.

Clearly a more extensive study could be made using numerical hydrocodes, in particular to study the fractionation of speeds and particle sizes within the expanding plume, but to a first order it seems that the expressions derived in the previous section for Earth and Venus, modified as above, can be used with reasonable confidence on Mars.

It is worth noting in passing that although the Moon has a negligible atmosphere, such that all impacts can be considered atmosphere-piercing, and would therefore distribute microtektites, it has a high typical impact velocity (~16 km/s). Thus much of the ejecta is accelerated to higher than escape speed (only 2.4 km/s) and is lost from the body. On Mars, the velocities are more favourable—the maximum ejecta speed $V_{\mathrm{i}}/2$ is only fractionally above the escape speed of 5 km/s, so relatively little material is lost from the planet.

Since we are considering global-scale distribution, the flat-Mars approximation is a poor one. Ballistic formulae (e.g., Bate *et al.* 1971) can be used, but a more graphic, interesting, and flexible approach is to model trajectories directly, since the trajectories of particles launched from a rotating planet can be remarkably complex (e.g., Dobrovolskis 1981).

TRAJECTORY AND HEATING MODELS

To study the trajectories of ejecta outside and at the edge of the atmosphere, particle trajectories are propagated using a trajectory code, implemented in the Interactive Data Language, developed for assessing spacecraft entry and descent trajectories and measurements. This code is available to other workers upon application to the author.

The state vector of the particle is stored as cartesian coordinates (X, Y, Z, Vx, Vy, Vz) where the origin of the coordinate system is the center of mass of the planet, the X axis joins the origin to the prime meridian and the equator, the Z axis is the north pole, and the Y axis completes a right-handed set.

The derivative of the state vector (i.e. velocity and acceleration) is computed from the drag and gravity forces, and the vector propagated forward using a 4th-order Runge–Kutta integrator, all in this Cartesian frame. The reference frame is rotated by the product of the planetary rotation rate and the time step, and the state vector is then recomputed in the rotated frame.

Planetary winds can be specified as zonal, meridional, and vertical components and converted into the particle frame. Winds are crucial in modeling the parabolic ejecta deposits on Venus where fall times of even large ejecta particles are long enough that winds can produce substantial horizontal displacements (Vervack and Melosh 1992, Schaller and Melosh 1998). However, in Mars' thin atmosphere, the fall times of >100-μm particles are only a couple of hours and planetary winds—much more complex on Mars in any case—can be largely ignored. Even at 20 m/s (a surface windspeed achieved at the height of the dust storms) a particle will move only 72 km in 2 h. Micrometer-sized ejecta will, like the dust in Mars' atmosphere today, remain for some time and be transported globally by winds, but this small material is not of interest in the present paper.

Entry heating is computed by an energy balance model, assuming the particles are isothermal (a reasonable assumption—the heating pulse is of the order of a few seconds, and particles considered are a millimeter or so in diameter at most and so have thermal conduction times $t \sim (a/\kappa)^{0.5}$ of 10 s or less, with κ the thermal diffusivity and a the diameter).

Following Fraundorf (1980), this model—originally due to Whipple—may be expressed

$$T^4 = T_{\mathrm{e}}^4 + 2.7 \times 10^{12} \Psi (m/A)(\cos\alpha/H) v^3, \qquad (11)$$

with m the particle mass in grams, T the peak temperature attained in K, T_{e} is the initial (radiative equilibrium) temperature in K, A the cross-sectional area of the particle in cm^2, H the atmospheric scale height in kilometers, and v the entry speed. Ψ is a constant, assumed unity, the fraction of the kinetic energy of impinging air molecules deposited onto the particle divided by the particle's emissivity. Entry angle is α, with $\alpha = 90^\circ$ vertical, giving peak heating. Since the objective of the calculation is to determine whether particles are melted or not, no ablation term is included, although note that for large (centimeter) particles, where the isothermal assumption would break down, this omission would be unacceptable. Since most particles of interest are >10 micrometers in diameter, and the temperatures of interest are >1000 K, the emissivity is assumed to equal unity. For very small particles, and if lower melting temperatures were of interest, again this would be a poor assumption—small particles are poor radiators.

RESULTS

Suborbital Trajectories

Figure 4 shows the loci of ejecta deposition for a fixed launch angle (45°) and various velocities for a launch site at 22°N, 87°W on Earth and Mars, chosen nominally as the site of the Chicxulub (K/T) crater on Earth. (There is, coincidentally, a large crater—Fesenkov, 86 km diameter—on Mars at this location, at the northeastern end of the Tharsis region). The contours are overlain for reference on the present-day continents of Earth and the USGS Viking Mars mosaic. Figure 4a may be compared with simulations of trajectories of ejecta from the K/T impact, as modeled in Alvarez (1990) and Argyle (1989), who give essentially equivalent results.

As might be expected, ejecta travels further for a given launch velocity around the planet on Mars than on Earth, since the escape velocity is lower and distances are smaller. Although the rotation periods of Earth and Mars are similar, the flight time of planet-traversing trajectories on Mars are longer compared

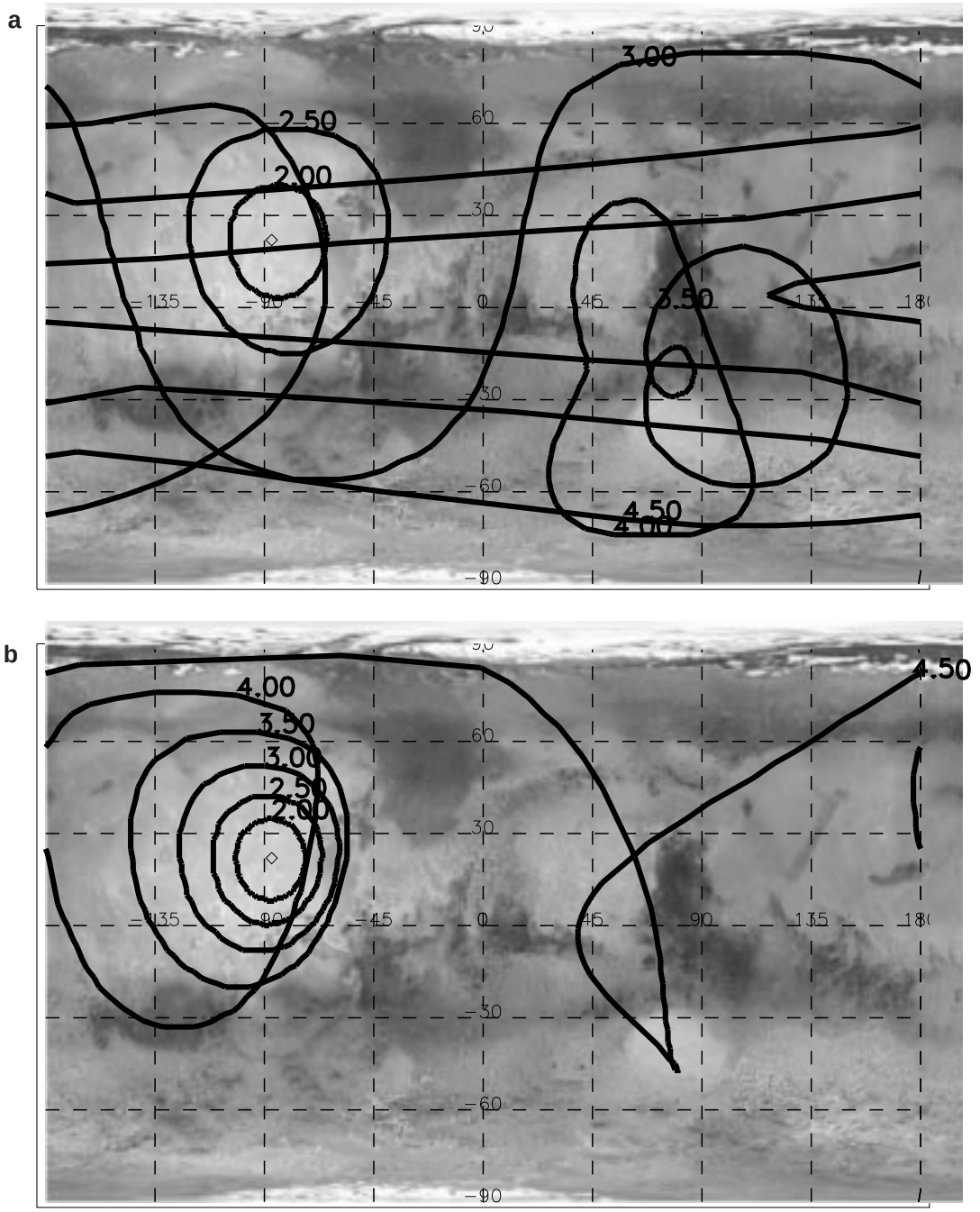

FIG. 5. As Fig. 4b, but for launch elevation angles of (a) 20° and (b) 70°. Note that for low launch angles ejecta travels somewhat further compared with the 45° case, and the contours tend to concentrate near the antipode of the impact.

with the rotation period, and so the loci on Mars are rather more distorted by planetary rotation than is the case for Earth. This may be seen in the long planet-girdling tail of the 4.5 km/s teardrop contour on Mars.

Figure 5 shows the same computation for launch angles of 20° and 70° on Mars. It can be seen that, depending on the launch angle, one or both poles may receive ejecta particles from impact events anywhere on the planet as long as the particles are launched at about 3–4 km/s. It may be noted that for shallow launch angles, the contours tend to converge at the antipode of the source crater—if equal amounts of ejecta are launched in each velocity bin, there may be a local increase in ejecta thickness away from the source crater. It should, however, be possible to discriminate this scenario from the more usual decrease away from the crater by studying the size distribution of particles—smaller particles tend to be thrown further from the crater.

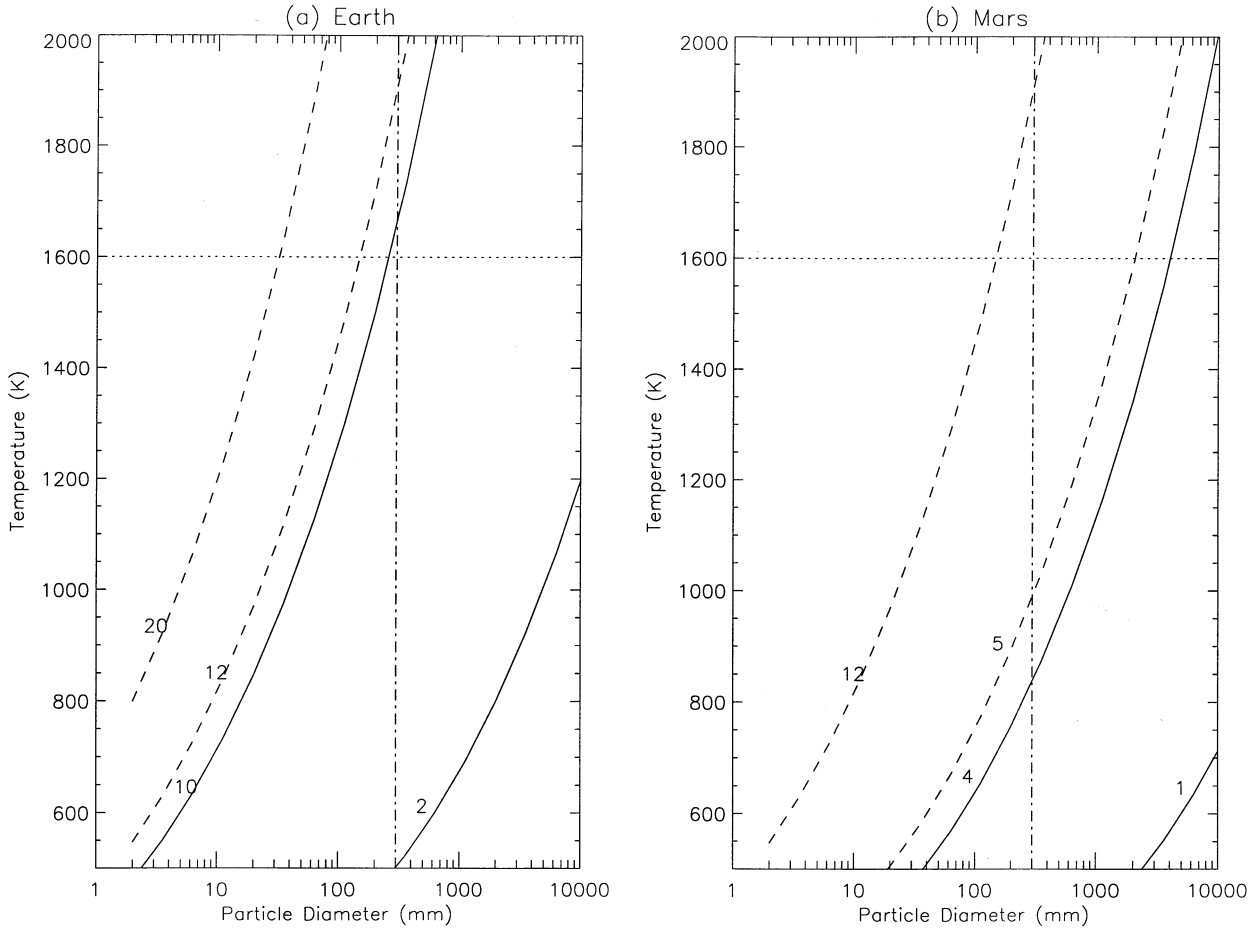

FIG. 6. Calculated entry temperatures for particles on Earth and Mars, assuming 90° entry angle. The dotted line indicates a typical silicate melting temperature—where the curves are above this line, entrant particles would melt. The solid curves indicate the likely velocity range for re-entrant ejecta (numbers indicate entry speed in km/s), while the dashed curves are for the most typical interplanetary impactors. The dash-dot line shows the size limit of spherical particles condensed from an impact vapor plume: ejecta particles to the left of this line are likely to have a molten appearance.

Particle Heating and Discrimination of Ejecta from IDPs

Heating of particles is radically different between Earth and Mars and is summarized in Fig. 6. On Earth, ballistically transported ejecta may be retained by the planet and yet still achieve temperatures of >1000 K. Indeed, such re-entrant ejecta was responsible for the ignition of global firestorms at the K/T boundary (Melosh *et al.* 1990). On Mars energetic ejecta is lost to space, while that which moves sufficiently slowly to be retained on suborbital trajectories has too little energy to melt on reentry. Since entry energy scales as radius^3, and radiating area as radius^2, larger particles of a given density and velocity reach higher temperatures.

It is seen that initially unmelted re-entrant particles must be several millimetres in diameter to reach melting point. Flynn and McKay (1990) compute the heating rates for meteors (i.e., IDPs) on Mars and find that, for a melting temperature of 1600 K, the expected velocity distribution at Mars, and a particle density of 1000 kg/m^3, virtually all 10-μm-diameter particles will be unmelted (as on Earth). Around 90% of 100-μm-diameter particles will be unmelted (compared with about 50% of those on Earth) and around 40% of 1-mm-diameter particles will be unmelted.

Many of the particles released from the impact vapor plume will have been condensed from it. Melosh and Vickery (1991) present a simple theory of the formation of spherules in impact plumes: they give the formula

$$r_\infty = 0.11 \frac{\sqrt{D_\mathrm{p}}}{v_\mathrm{i}}, \qquad (12)$$

with D_p and v_i the impactor diameter and velocity, respectively, as in Eq. (1), and r_∞ the radius of the typical spherule formed by the balance of aerodynamic shear and droplet surface tension. For an impactor of 200 m radius or so and a 10 km/s impact velocity, this leads to $r_\infty \sim 150$ μm. Many smaller droplets will also be present (although these are more likely, perhaps, to be expelled from the martian gravity well since those particles of this size that survive and are not incorporated into larger particles must be in the outer, higher-energy part of the plume).

Figure 6 shows the peak temperatures attained by particles entering the atmospheres of Mars and Earth (assuming $\alpha = 90^\circ$ and $H = 8$ km, although the results are not particularly sensitive to these parameters). For velocities on Earth smaller than the escape speed, all sub-centimeter particles larger than those likely (Eq. (12)) to have been produced in the vapor plume remain cooler than the melting point, whereas particles on hyperbolic trajectories (i.e., meteoric material) larger than about 10 μm will melt. Thus on Earth, melting does not discriminate ~300-μm-diameter particles between meteoric and impact sources. On Mars, on the other hand, the low escape speed makes a convenient distiction—the high-velocity meteor curve crosses the melting point close to the ejecta plume size threshold.

Examining the velocity distribution of Flynn and McKay (1990) it can be seen that only 20% of incoming particles exceed 12 km/s; thus the vast majority of meteoric particles smaller than 300 μm diameter will remain unmelted. On the other hand, molten particles of this size range and smaller will be produced in an impact vapor plume.

Thus the size distributions of molten ejecta particles, and molten IDPs are somewhat complementary—if most of the 100- to 300-μm particles in a sample are molten, this is strong circumstantial evidence that these particles are derived from ejecta.

There exist additional thermometers in particles, beyond morphological evidence of melting; these are discussed in detail in Flynn (1989) but summarized here. Close examination by transmission electron microscopy could identify solar flare tracks—these would be present only in IDPs and only those IDPs whose temperatures did not reach 900 K or so; at this temperature tracks are annealed in times comparable with the duration of the atmospheric heating pulse. Heating to similar temperatures is likely to cause dehydration of minerals, and might be detectable in near-IR spectra. Temperatures of 900 K lead to substantial loss of zinc, while particles heated above 1200 K are likely to lose sulfur (a notably abundant element in martian soil. Collectively, these indicators should be able to discriminate between particles heated to $\gg$900 K and those not.

An additional feature of microspherules derived from ejecta plumes is that the relatively large number density of particles within the plume allows for the possibility of interparticle collisions (the mechanisms by which many particles grow in the earlier, hotter stage of the plume expansion, like raindrops in a cloud, to the size limit given above). Evidence of these collisions has been seen in the Australian microtektites, some of which themselves bear tiny impact craters (Prasad and Sudhakar 1998). IDPs are far less likely to encounter such collisions.

CRATERING RATE AND EJECTA LAYERS ON MARS

The impact cratering rate on Mars, as elsewhere, is a subject of controversy. Neukum and Ivanov (1994) compute from the orbital dynamics of asteroids that the interval between Meteor Crater (10^{18} J, 1 km) events should be around 1600 years for the whole Earth (6000 years for the continents). For 100-km craters, the interval should be around 27 Myr for the whole Earth.

Hughes (1999) finds a 15 Myr interval between 100-km "dry land" cratering events—or a rate ~6 times higher. Morrison *et al.* (1994) find that 60- to 125-km craters should occur on Earth every 1–4 Myr, a rate higher still, while 12- to 30-km craters occur every 63–300 kyr. This latter terrestrial rate is similar to that derived by Grieve and Pesonen (1992) and Grieve and Shoemaker (1994) who find that the geological record suggests that 20-km craters form at a rate of about 5×10^{-15} km^{-2} year^{-1}, or about every 400 kyr.

Neukum and Ivanov (1994) suggest that both Earth and Mars have cratering rates for crater diameters of 1 km diameter of about 0.6 times the lunar rate. Their curves show for 10-km-diameter craters that the Earth rate is about 1.5 times that of the Moon, whereas for Mars it is only about 1.2 times that of the Moon.

Table 2 in Barlow (1990) suggests that the martian crater density is about equal to that of the Moon, while Strom *et al.* (1992), following the Basaltic Volcanism Study Project (1981) suggest that the martian cratering rate may be between 1 and 4 times the lunar rate, with twice the lunar rate being the most likely value (the ratio depends on the fraction of craters that are assumed to be due to comets instead of asteroids: a higher asteroidal population increases the relative impact rate at Mars).

In summary, the uncertainties in scaling the lunar or terrestrial cratering rates to Mars are rather less than the uncertainties in the absolute values of these rates. Taking all the above into consideration, it seems likely that 1-km craters form on Mars every 3000–10,000 years. A K/T (10^{24} J, ~130 km diameter) type impact should occur every 10^8 years or so and a Zhamanshin (10^{20} J, 15 km diameter)-sized crater every 10^6 years.

It follows that craters able to pierce the atmosphere and form microtektite layers, i.e., forming craters >3 km in diameter, would therefore be expected on Mars about once every 10^4–10^5 years. Thus, taking the ice deposition rate earlier, one may expect ejecta layers every few meters to tens of meters. If such a minimum size crater were to form near the equator, the ejecta layer in the polar terrain would be very thin, ~10^{-9} m, or about 1 particle every 10 cm^2. A 15-km crater, similarly distant, would give several particles every square centimeter—certainly detectable in a careful search. Craters closer to the area under investigation will obviously produce thicker layers.

The strong dependence of ejecta volume on crater diameter should be borne in mind: the 220-km crater Lyot, for example, is moderately young (Garvin, personal communication) and at 50°N is ~2400 and ~7700 km from the north and south poles, respectively. The expected ejecta thicknesses at the poles for this event are 4 cm and 1 mm—both should be quite apparent to even a cursory inspection with suitable instrumentation.

As on Earth, glaciological processes may concentrate particles for collection and inspection. Where different layers are exposed by flow or ablation in the ice cap, a number of ejecta layers may be easily accessible to investigation.

Although the ice caps themselves offer the most likely prospects for preservation and recognition of microtektites, the extensive layered terrains should also retain ejecta layers, although probably with a much higher dust content. In this environment, the microtektites may suffer more abrasion than in the ice, and so may not look as glassy. However, as noted earlier, the bulk of the airborne dust—and thus probably the bulk of the material in the layers—is very much smaller than the typical microtektite particles discussed in this paper, which may allow discrimination of the latter.

PROSPECTS FOR OBSERVATIONS

Future Mars missions may carry a ground-penetrating radar which may be able to resolve layers in the martian surface (Plaut 1998). One aspect of a layer that might lend credence to an impact ejecta origin is a thickness variation that follows a dependence with distance from a known impact crater like those relationships plotted in Fig. 2. It is not clear to what extent layers may be evident in radar profiles of martian ice layers, since their temperature and composition (CO_2-rich) are very different from those of the terrestrial ice sheets. Further, the main mechanism for horizon formation on Earth is via enhanced electrical conductivity through raised sulfate concentration. Ejecta layers on Mars may not have such ionic activity, and may be too thin in general to permit a strong reflection due to dielectric contrast alone. In any case, the overall dust content of the martian caps may limit radar sounding to shallow layers, and inhibit the discrimination of ejecta layers.

In situ inspection by microscope of exposed columns (either from trenches or boreholes, or the edges of scarps or crevasses) should give a broad characterization of the size distribution of particles, their morphology (and thus the fraction of them that have been melted), and perhaps, via multispectral imaging, of their gross mineralogy. Ejecta particles can be easily concentrated by melting/evaporating the ice component of a sample. These observations should enable the identification of ejecta layers. The imaging results from the Remote Arm Camera on the Mars Polar Lander are therefore eagerly awaited; with $\sim$25-μm pixels (Keller *et al.* 1999) it should be quite possible to recognize $\sim$300-μm-diameter particles as being round. With appropriate lighting, it may even be possible to identify such particles as having a glassy texture.

Although the 1998 Mars Polar Lander does not have elemental composition instrumentation, if an ejecta layer were found, the Thermal and Evolved Gas Analyzer (TEGA) instrument on board could at least establish whether the material released volatiles on heating—ejecta should already have been devolatilized during its formation.

The ultimate prospects for investigating ejecta layers lie in taking ice cores on Mars. Very high magnification, beyond conventional optical microscopy and near-term *in situ* robotic capabilities (but well within the routine capabilities of sample analysis laboratories on Earth) may yield further insights, notably the existence of craters on the particles.

If samples are taken at several locations, and the same contiguous ejecta layer is recognized, it may be possible to identify the source crater by regressing the layer thickness to distance from the source crater, as for the suspected Southeast Asia crater on Earth (Glass and Pizzuto 1994). If the layer is shallow, i.e., very recent, it may be possible to identify the source crater directly from remote sensing evidence of the crater's young age.

The age of the ice caps is not well-known, and although the surfaces may be young, deep material could have an age considerably older than the few Myr assumed in this paper. The more widespread and older layered terrain probably has a good stratigraphic record, although evidently a much higher dust content. Furthermore, the properties explored in this paper may be preserved by particles in other sedimentary records, for example lake sediments. A record of impact ejecta covering extensive periods of time may be present. If this is the case, investigations beyond the simple search for ejecta layers and insight into the ejecta distribution process become exciting possibilities. For example, various investigators have proposed (but so far have not convincingly demonstrated) a periodicity in the cratering record on Earth.

CONCLUSIONS

1. The propensity for global ballistic transport of ejecta on Mars has been noted, due to the low atmospheric pressure making the atmosphere easy to puncture, and the small gravity and radius making the velocity requirements for global transport quite small.

2. The variability of distal ejecta thickness vs distance from the source crater has been reviewed, and although there are substantial uncertainties, the expression (derived from near-field ejecta) by McGetchin *et al.* (1973) performs well for terrestrial microtektite fields. The volume of Venus' parabolic ejecta deposits are similarly well-described; the expression is closely related to an independent formula for crater melt volume due to Grieve and Cintala (1992) and to observations on the melt/dust content of plumes from nuclear explosions.

3. Consideration of typical impact velocities suggests that ejecta volumes are somewhat ($\sim$2.5$\times$) lower for Mars craters of a given size than for those on Earth, but—unlike for the Moon—the ejecta velocities are low enough that most of the ejecta is retained. The distance dependence of ejecta thickness should be the same for Mars as for Earth.

4. Consideration of the volume and dispersal of ejecta suggest that it is likely that impact events expected to have occurred somewhere on Mars in the last few Myr (the estimated age of the polar caps) will produce layers of ejecta material with particle densities large enough to be detected *in situ*. It should be noted, however, that larger impacts produce dramatically more ejecta volume.

5. Modeling of the atmospheric heating of incoming meteoric material suggests that in general the size ranges of particles

likely to melt during entry are above a few hundred micrometers in diameter. All re-entrant ejecta particles below ~5 mm in diameter are likely to survive unmelted; however, large numbers of droplets around 300 μm in diameter and smaller would be expected to have condensed from or frozen from melt inside the expanding ejecta plume. Thus the combination of size distribution, melt morphology, and other indicators such as composition and microimpact craters are likely to make identification of ejecta particles moderately straightforward.

6. Instrumentation on near-term Mars missions offers uncertain prospects—serendipitous discovery of an impact layer at the Mars Polar Lander site is quite possible, and future ground-penetrating radars may be able to identify layers as likely candidates. As a long-term objective, coring analysis of the martian ice caps is all but certain to identify such layers. Whether detailed analysis of martian ice cores will occur in human-operated laboratories on Mars, or the cores are instead returned to Earth is an interesting question that only the future can answer.

ACKNOWLEDGMENTS

The idea for this paper arose during discussions at the Mars Polar Science and Exploration Conference in Texas, October 1998: the author thanks the organizers of that meeting for orchestrating such a stimulating gathering. The trajectory code was developed with the support of the Cassini Project with encouragement of the Huygens Science Working Team. Referees Jim Garvin and Nadine Barlow are thanked for helpful suggestions: Garvin in particular suggested a fruitful direction of further enquiry. Useful discussions with Jay Melosh are also acknowledged.

REFERENCES

Adushkin, V. V., and I. V. Nemchinov 1994. Consequences of impacts of cosmic bodies on the surface of the Earth. In *Hazards Due to Comets and Asteroids* (T. Gehrels, Ed.), pp. 721–778. Univ. of Arizona Press, Tucson.

Alvarez, W. 1990. Trajectories of ballistic ejecta from the Chicxulub Crater. *Geol. Soc. Am. Spec. Pap.* **247**, 141–150.

Argyle, E. 1989. Global fallout signature of the K/T Bolide. *Icarus* **77**, 220–222.

Barlow, N. G. 1990. Application of the inner Solar System cratering record to the Earth. *Geol. Soc. Am. Spec. Pap.* **247**, 181–187.

Basaltic Volcanism Study Project 1981. *Basaltic Volcanism on the Terrestrial Planets.* Pergamon, New York.

Bate, R. R., D. D. Mueller, and J. E. White 1971. *Fundamentals of Astrodynamics.* Dover, New York.

Blasius, K. R., J. A. Cutts, and A. D. Howard 1982. Topography and stratigraphy of martian polar layered deposits. *Icarus* **50**, 140–160.

Campbell, D. B., N. J. S. Stacy, W. I. Newman, R. E. Arvidson, E. M. Jones, G. S. Musser, A. Y. Roper, and C. Schaller 1992. Magellan observations of extended impact crater related features on the surface of Venus. *J. Geophys. Res.* **97**, 16,249–16,277.

Cintala, M. J., and R. A. F. Grieve 1991. Impact melting and peak-ring basins: Interplanetary considerations. *Proc. Lunar Planet. Sci. Conf. 22nd*, 215–216. [Abstract]

Clifford, S. M., M. J. Cintala, and N. G. Barlow 1991. An estimate of the global thickness of impact melt on Mars. *Proc. Lunar Planet. Sci. Conf. 22nd*, 223–224. [Abstract]

Croft, S. K. 1985. The scaling of complex craters. *Proc. Lunar Planet. Sci. Conf. 8th*, 828–842.

Cutts, J. A., K. R. Blasius, G. A. Briggs, M. H. Carr, R. Greeley, and H. Masursky 1976. North polar region of Mars: Imaging results from Viking 2. *Science* **194**, 1329–1337.

Dobrovolskis, A. 1981. Ejecta patterns diagnostic of planetary rotations. *Icarus* **47**, 203–219.

Flynn, G. J. 1989. Atmospheric entry heating: A criterion to distinguish between asteroidal and cometary sources of interplanetary dust. *Icarus* **77**, 287–310.

Flynn, G. J., and D. S. McKay 1990. An assessment of the meteoric contribution to the martian soil. *J. Geophys. Res.* **95**, 14,497–14,509.

Fraundorf, P. 1980. The distribution of temperature maxima for micrometeorites decelerated in the Earth's atmosphere without melting. *Geophys. Res. Lett.* **10**, 765–768.

Garvin, J. B., and J. J. Frawley 1998. Geometric properties of martian impact craters: Preliminary results from the Mars Orbiter Laser Altimeter. *Geophys. Res. Lett.* **25**, 4405–4408.

Gersonde, R., F. T. Kyte, U. Bleil, B. Deikmann, J. A. Flores, K. Gohl, G. Grahl, R. Hagen, G. Kuhn, F. J. Sierro, D. Volker, A. Abelmann, and J. A. Bostwick 1997. Geological record and reconstruction of the late Plioceme impact of the Eltanin asteroid in the Southern Ocean. *Nature* **390**, 357–363.

Glass, B. P. 1990. Tektites and microtektites: Key facts and inferences. *Tectonophysics* **171**, 393–404.

Glass, B. P., and J. E. Pizzuto 1994. Geographic variation in Australian microtektite concentrations: Implications concerning the location and size of the source crater. *J. Geophys. Res.* **99**, 19,075–19,081.

Grieve, R. A. F., and M. J. Cintala 1992. An analysis of differential impact melt-crater scaling and implications for the terrestrial impact record. *Meteoritics* **27**, 526–538.

Grieve, R. A. F., and M. J. Cintala 1998. Planetary impacts. In *Encyclopedia of the Solar System* (P. R. Weissman, L.-A. McFadden, and T. V. Johnson, Eds.), pp. 845–876. Academic Press, San Diego.

Grieve, R. A. F., and L. J. Pesonen 1992. The terrestrial impact cratering record. *Tectonophysics* **216**, 1–30.

Grieve, R. A. F., and E. M. Shoemaker 1994. The record of past impacts on Earth. In *Hazards Due to Comets and Asteroids* (T. Gehrels, Ed.), pp. 417–462. Univ. of Arizona Press, Tucson.

Herkenhoff, K. E., J. J. Plaut, and S. A. Nowicki 1997. Surface age and resurfacing rate of the north polar layered terrain on Mars. *Proc. Lunar Planet. Sci. Conf. 28th*, 551–552. [Abstracts]

Hildebrand, A. R. 1992. *Geochemistry and Stratigraphy of the Cretaceous/Tertiary Boundary Impact Ejecta*. Ph.D. dissertation, University of Arizona, Tucson.

Hildebrand, A. R., and J. A. Stansberry 1992. K/T boundary ejecta distribution predicts size and location of Chicxulub Crater. *Proc. Lunar Planet. Sci. Conf. 13th*, 537–538. [Abstract]

Hughes, D. W. 1999. The cratering rate of planet Earth. *J. Br. Interplanet. Soc.* **52**, 83–94.

Keller, H. U., H. Hartwig, R. Kramm, D. Koschny, W. J. Markiewicz, N. Thomas, M. Fernandez, P. Smith, R. Reynolds, and J. Weinberg 1999. The MVACS robotic arm camera. *J.Geophys. Res.*, in press.

McGetchin, T. R., M. Settle, and J. W. Head 1973. Radial thickness variation in impact crater ejecta: Implications for lunar basin deposits. *Earth Planet. Sci. Lett.* **20**, 226–236.

Melosh, H. J. 1989. *Impact Cratering—A Geologic Process.* Oxford Univ. Press, London.

Melosh H. J., and A. M. Vickery 1991. Melt droplet formation in energetic impact events. *Nature* **350**, 494–496.

Melosh, H. J., N. M. Schneider, K. Zahnle, and P. Latham 1990. Ignition of global wildfires at the Cretacious/Tertiary boundary. *Nature* **343**, 251–254.

Moersch, J. E., J. F. Bell III, T. L. Hayward, S. W. Squyres, J. Van Cleve, S. Lee, and L. M. Carter 1999. Regional dust deposition rates on Mars from time-variable thermophysical properties of the surface. *Icarus*, submitted.

Morrison, D., C. Chapman, and P. Slovic 1994. The impact hazard. In *Hazards Due to Comets and Asteroids* (T. Gehrels, Ed.), pp. 59–91. Univ. of Arizona Press, Tucson.

Neukum, G., and B. A. Ivanov 1994. Crater size distributions and impact probabilities on Earth from lunar, terrestrial-planet, and asteroid cratering data. In *Hazards Due to Comets and Asteroids* (T. Gehrels, Ed.), pp. 359–416. Univ. of Arizona Press, Tucson.

Plaut, J. J. 1998. The Mars express subsurface sounding radar: Water and ice detection in the polar regions. *Abstracts, 1st International Conference on Mars Polar Science and Exploration*, LPI Contribution 953, pp. 31–32.

Plaut, J. J., R. Kahn, E. A. Guinness, and R. E. Arvidson 1988. Accumulation of sedimentary debris in the south polar region of Mars and implications for climate history. *Icarus* **75**, 357–377.

Prasad, M. S., and M. Sudhakar 1998. Microimpact phenomena on Australasian microtektites: Implications for ejecta plume characteristics and lunar surface processes. *Meteoritics Planet. Sci.* **33**, 1271–1279.

Robin, E., L. Froget, C. Jehanno, and R. Roccia 1993. Evidence for a K/T impact in the Pacific Ocean. *Nature* **365**, 615–617.

Schaller, C. J., and H. J. Melosh 1998. Venusian ejecta Parabolas: Comparing theory with observations. *Icarus* **131**, 123–137.

Schmidt, R. M., and K. R. Housen 1987. Some recent advances in the scaling of impact and explosion cratering. *Int. J. Impact Eng.* **5**, 543–560.

Smit, J. 1997. The big splash. *Nature* **390**, 340–341.

Stoffler, D., D. E. Gault, J. Wedekind, and G. Polkowski 1975. Experimental hypervelocity impact into quartz sand: Distribution and shock metamorphism of ejecta. *J. Geophys. Res.* **80**, 4062–4077.

Strom, R. G., S. K. Croft, and N. Barlow 1992. The martian impact cratering record. In *Mars* (H. H. Keiffer, B. M. Jakosky, C. W. Snyder, and M. S. Matthews, Eds.), pp. 383–423. Univ. of Arizona Press, Tucson.

Thomas, P. C., and P. J. Gierasch 1995. Polar margin dunes and winds on Mars. *J. Geophys. Res.* **100**, 5397–5406.

Thomas, P., S. Squyres, K. Herkenhoff, A. Howard, and B. Murray 1992. Polar deposits of Mars. In *Mars* (H. H. Keiffer, B. M. Jakosky, C. W. Snyder, and M. S. Matthews, Eds.), pp. 767–798. Univ. of Arizona Press, Tucson.

Tomasko, M. G., L. R. Doose, M. Lemmon, P. H. Smith, and E. Wegryn 1999. Properties of dust in the martian atmosphere from the imager on Mars Pathfinder. *J. Geophys. Res.* **104**, 8987–9008.

Toon, O. B., K. Zahnle, D. Morrison, R. P. Turco, and C. Covey. 1997. Environmental perturbations caused by the impact of asteroids and comets. *Rev. Geophys.* **35**, 41–78.

Toon, O. B., K. Zahnle, R. P. Turco, and C. Covey 1994. Environmental perturbations caused by asteroid impacts. In *Hazards Due to Comets and Asteroids* (T. Gehrels, Ed.), pp. 791–826. Univ. of Arizona Press, Tucson.

Vervack, R. J., Jr., and H. J. Melosh 1992. Wind interaction with falling ejecta: Origin of the parabolic features on Venus. *Geophys. Res. Lett.* **19**, 525–528.

Vickery, A. M., and H. J. Melosh 1990. Atmospheric erosion and impactor retention in large impacts with application to mass extinctions. *Geol. Soc. Am. Spec. Pap.* **247**, 289–300.

Zahnle, K. 1990. Atmospheric chemistry by large impacts. *Geol. Soc. Am. Spec. Pap.* **247**, 391–400.

Zuber, M. T., D. E. Smith, S. C. Solomon, J. B. Abshire, R. S. Afzal, O. Aharonson, K. Fishbaugh, P. G. Ford, H. V. Frey, J. B. Garvin, J. W. Head, A. B. Ivanov, C. L. Johnson, D. O. Muhleman, G. A. Neumann, G. H. Pettengill, R. J. Phillips, X. Sun, H. J. Zwally, W. B. Banerdt, and T. C. Duxbury 1998. Observations of the north polar region of Mars from the Mars Orbiter Laser Altimeter. *Science* **282**, 2053–2060.